

HOMOGENEOUS LATTICE DISORDER AND SUPERCONDUCTING
PROPERTIES OF $\text{YBa}_2\text{Cu}_3\text{O}_{6.9}$ FILMS

DAVOR PAVUNA and ANDREA GAUZZI¹

*Department of Physics, Swiss Federal Institute of Technology at Lausanne (EPFL),
CH - 1015 Lausanne, Switzerland*

Dedicated to Professor Mladen Paić on the occasion of his 90th birthday

Received 27 June 1995

UDC 538.945, 539.213

PACS 61.43.-j, 74.76.-w, 74.62.Dh

We discuss the striking changes of the superconducting properties of $\text{YBa}_2\text{Cu}_3\text{O}_{6.9}$ films to the homogeneous lattice disorder, induced by varying growth temperatures: T_c decreases with increasing disorder, while the width of the resistive transition and the normal state resistivity increase. We estimate the length scale of such disorder from the broadening $\Delta\theta$ of the $\langle 005 \rangle$ X-ray diffraction rocking curves. The suppression of superconductivity and normal conductivity scales as $\Delta\theta$ and appears for in-plane lattice coherence lengths $r_c \approx 1/\Delta\theta$ smaller than about 10 nm.

1. Introduction

The prevailing ideas in the research on superconducting cuprates assign to oxygen doping (and to atomic substitutions) the predominant role in controlling the superconducting and the normal state of these solids. Recent experimental and

¹Present address: Ecole Supérieure de Physique et Chimie Industrielles de la Ville de Paris (ESPCI), Laboratoire de Physique du Solide (LPS), 10, Rue Vauquelin 75231 Paris 05 Cedex, France.

theoretical studies give some evidence for a percolative or phase-separated picture of superconductivity, which implies that electronic and structural properties on the atomic scale play an equally important role. These properties vary randomly over long distances, since their spatial correlation is dominated by the range of the interatomic forces. In $\text{YBa}_2\text{Cu}_3\text{O}_{6+x}$ (YBCO), for example, experimental data on quenched samples [1] give evidence that the superconducting and normal properties are sensitive not only to the average oxygen content x , but also to the degree of oxygen order on the *local* (nm) scale. This experimental evidence is supported by numerical simulations [2] and by the predictions of the microscopic charge transfer model [3]. Detailed analysis of short-range structural order in cuprates is, therefore, required in order to fully understand their electronic and superconducting properties.

The aforementioned type of disorder exists independently from the disorder introduced by the grain structure (if any). According to Deutscher et al. [4], the first type of disorder (“homogeneous”) induces localization and suppresses superconductivity. The second type of disorder (“granular”) reduces significantly the critical current density [5], since superconductivity occurs as a percolation through the network of grains. In the first case, the characteristic length of the disorder is the lattice coherence length r_c , i.e. the characteristic length scale over which atomic positions are correlated. In the second (“granular”) case the relevant parameters for the disorder are the grain size and the angular distribution of the grains.

We have systematically studied the effects of growth temperature on the electrical and structural properties of YBCO films. We have found that the growth induces “static” lattice disorder which is surprisingly “homogeneous”. Such disorder affects strikingly both, the superconducting transition and the conductivity.

In this article we show that homogeneous lattice disorder can be quantitatively analysed and correlated with electronic properties. We estimate the variation of the in-plane lattice coherence length r_c from the broadening of the $\langle 005 \rangle$ X-ray diffraction rocking curves measured on our samples. We establish a quantitative correlation between r_c and the broadening of the superconducting transition as well as the behaviour of the normal state conductivity.

2. *Experimental techniques*

A complete description of our ion beam sputtering technique is given elsewhere [6]. The simplified system consists of a 3 cm diameter Kaufman Ar^+ source directed on a 10 cm diameter stoichiometric “123” target (see Fig. 1). We use beam voltage of 500 eV and beam current of 20 mA. These beam conditions are necessary to achieve the stoichiometric transfer from the target to the films; note that our deposition rate is extremely low (about 0.05×10^{-10} m/s). To allow the tetragonal to ortho-II ($x \approx 0.5$) phase transformation of the films, the chamber is backfilled with oxygen after deposition, while the substrate temperature T_{sub} is kept constant for 5 minutes. To favour the formation of the ortho-I phase ($x \approx 0.9$) during the cooling down of the substrates, a second dwell of 45 minutes is performed at 450 °C.

As-deposited films were measured by “standard” resistivity and critical current density techniques, X-ray diffraction analysis, Auger electron spectroscopy (AES), scanning electron microscopy (SEM) and stylus profilometry.

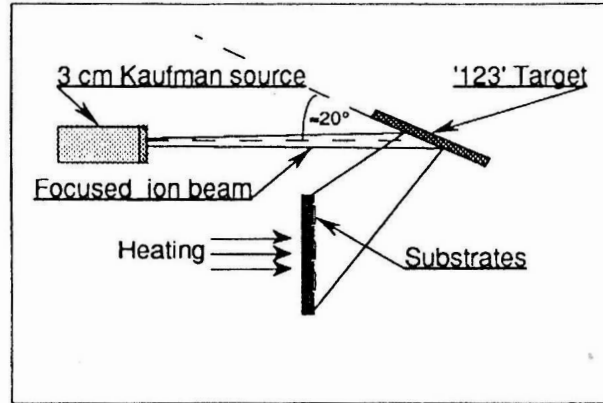


Fig. 1. Schematic diagram of the versatile mono-target ion beam sputtering technique developed by our group at the Ecole Polytechnique in Lausanne.

The main results were obtained on a series of about 50 nm thick films deposited on $\langle 001 \rangle$ SrTiO_3 at different temperatures; all other deposition parameters were unchanged. For $630 < T_{sub} < 700$ °C, the as-deposited films are c -axis oriented and epitaxial with a or b axis parallel to the a axis of the $\langle 001 \rangle$ SrTiO_3 substrate. Only the films grown in the narrow range $T_{sub} \approx (675 \pm 5)$ °C exhibit the typical properties of the ortho-I phase (see Fig. 2): zero-resistance critical temperature $T_{c0} \approx (90 \pm 1)$ K; $\Delta T_c < 1$ K; room temperature in-plane resistivity $\rho_{ab}(300 \text{ K}) = (250 \pm 50)$ $\mu\Omega\text{cm}$; $\rho_{ab}(300 \text{ K})/\rho_{ab}(100 \text{ K}) = 2.9 \pm 0.1$; residual resistivity extrapolated to 0 K $\rho_{res} = (0 - 10)$ $\mu\Omega\text{cm}$ (see Fig. 3). In the films grown at higher or lower temperatures, T_c decreases, while ΔT_c and $\rho_{ab}(300 \text{ K})$ increase, rapidly. The increase of $\rho_{ab}(300 \text{ K})$ is accompanied by an increase of ρ_{res} and by the appearance of a progressively large downward curvature in the temperature dependence of ρ_{ab} [7].

The optimal growth temperature is narrower in our case than for other film deposition techniques, such as laser ablation. This difference is possibly due to the lower growth temperatures, lower deposition rate and lower oxygen partial pressure that are characteristic of our mono-target ion beam sputtering technique.

3. Results and discussion

To account for the above effects of the growth temperature, we have carried systematic X-ray diffraction studies and rocking curve analyses of the $\langle 005 \rangle$ reflections from YBCO films. As soon as T_{sub} deviates from 675 °C, we have observed four characteristics: i) for all the $\langle 00l \rangle$ peaks, both the integrated and maxi-

imum diffraction intensities are progressively reduced; ii) the relative intensities of the $\langle 001 \rangle$ peaks are unchanged; iii) the rocking curve becomes progressively larger (see Fig. 4); iv) the shape of the rocking curve is in all cases described within the experimental error by a simple Lorentzian function (see Fig. 3).

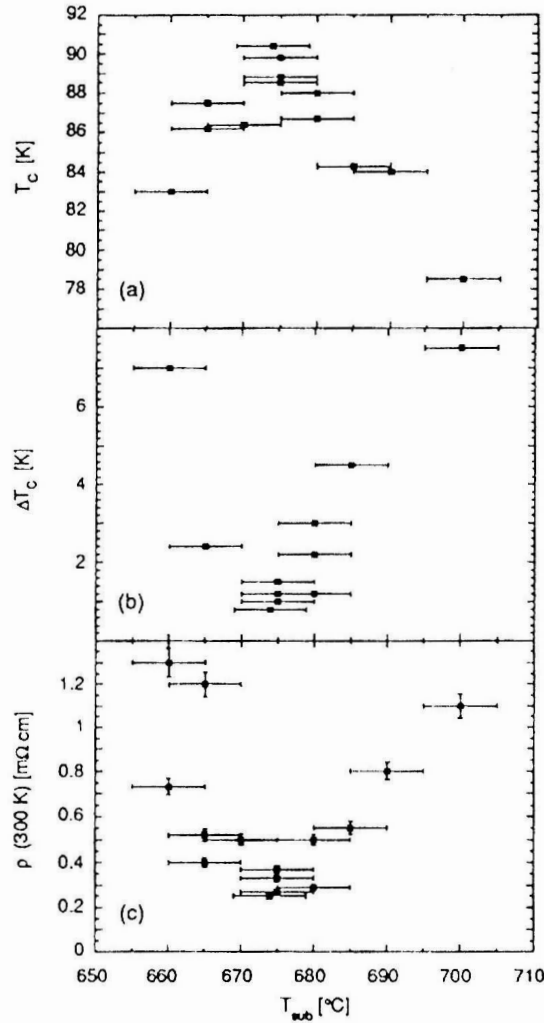


Fig. 2. (a) Dependence of the superconducting transition temperature T_c , (b) width of the resistive transition ΔT_c and (c) in-plane room temperature resistivity ρ_{ab} (300 K), on growth temperature T_{sub} (temperature of the substrate holder) for a series of YBCO films. T_c is defined as the intersection of the tangent to the transition curve at the midpoint with the temperature axis, while ΔT_c is defined as the full width at half maximum of the peak of the temperature derivative of the resistivity curve.

Based on the second observation (ii), we exclude the possibility that the films with reduced T_c are oxygen deficient ($x < 0.9$), since there exists a well-defined correlation between x and the relative intensities of the $\langle 001 \rangle$ reflections [8]. Furthermore, in agreement with the results of Nakamura et al. [9], we have found that an initial dwell of 5 minutes after deposition under an oxygen partial pressure of about 150 Pa is sufficient to obtain $T_{c0}^s \approx 90$ K and sharp transitions in the films grown at the optimal temperature. Longer dwells (of up to 20 minutes for the first one and up to 60 minutes for the second one at 450 °C) and/or higher oxygen partial pressures (up to about 10^4 Pa) during the first dwell do not affect any film property, independently of the growth temperature. This confirms that full oxidation is achieved rapidly, within a few minutes in all our 50 nm thick films.

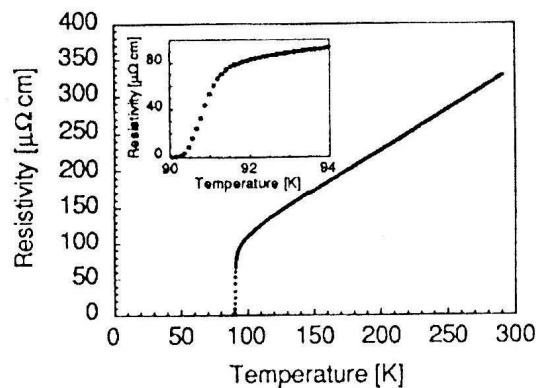


Fig. 3: Temperature dependence of resistivity of 50 nm thick $\text{YBa}_2\text{Cu}_3\text{O}_{6.9}$ film grown on $\langle 001 \rangle$ SrTiO_3 by single-target ion-beam sputtering at $T_{sub} \approx (675 \pm 50)$ °C.

We exclude the possibility that the broadening of the rocking curves is due to the mosaic spread. If this were the case, the integrated diffraction intensities would be constant, contrary to the observation (i). Further, the shape of the rocking curve would be described by a Gaussian function, contrary to our observation (iv), since the statistical distribution of the spread would be uncorrelated in space [10]. We note that the Gaussian broadening is indeed observed in laser ablated films, as reported by Wooldridge et al. [11]. Thirdly, and according to the discussion briefly given in the Introduction, no significant alteration of T_c and ρ would be observed.

The reduction of the central diffracted intensity of the rocking curves provides evidence that the broadening of these curves is due to the reduction of long range order in the lattice, or more loosely, by the increase in the “static” disorder induced by imperfect growth. This conclusion is supported by the appearance of a downward curvature in the temperature-dependence of the resistivity that increases with increasing resistivity: the disorder reduces the mean free-path of the carriers and enhances localization effects. The above feature of the resistivity is precisely the signature of the saturation of the scattering cross-section of the carriers due to a

short mean free-path as discussed in Ref. 12.

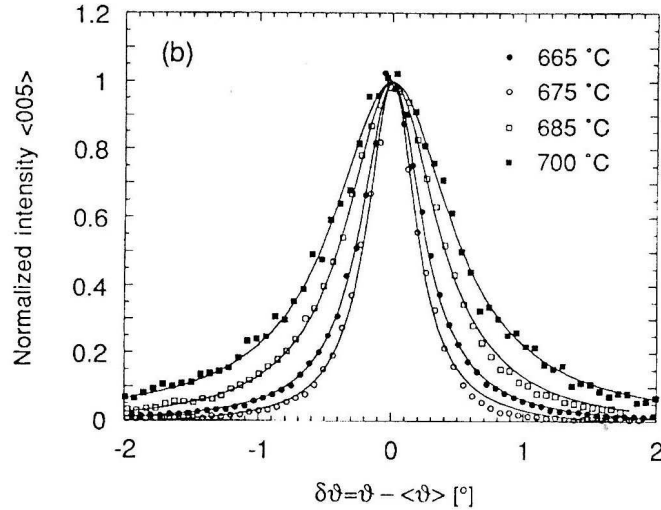


Fig. 4. Comparison between the broadening of the $\langle 005 \rangle$ Bragg reflexion of YBCO in films grown at different temperatures indicated by the legend. The solid lines represent Lorentzian fits of the experimental points.

4. Lattice coherence length

We estimate the characteristic length of the disorder in our films from the experimental broadening of the $\langle 005 \rangle$ rocking curve. Within the framework of the simple kinematical theory of diffraction, which is suited for our disordered thin films, the diffracted intensity at the Bragg angle ϑ of a given reflection is proportional to the structure factor $S[\vec{q}(\vartheta)]$ of this reflection. In all our films, the shape of the rocking curves is Lorentzian. Since S is the inverse Fourier transform of the self-correlation (or Patterson) function $G(\vec{r})$ of the electron density, it follows that $G(\vec{r}) \sim \exp(-|\vec{r}|/r_c)$, where r_c is the lattice coherence length. For our c -oriented films, taking into account the geometrical arrangement of the measurement, \vec{r} lies in the ab -plane. Straightforward calculation gives the following relation between r_c and the full width at half maximum $\Delta\vartheta$ of the rocking curve:

$$r_c = \frac{1}{\pi} \frac{d}{l\Delta\vartheta}, \quad (1)$$

where $d = 1.169$ nm is the c -axis lattice parameter of YBCO and l is the order of the $\langle 00l \rangle$ Bragg reflection. In Fig. 5 we present the experimental correlation between T_c and r_c . We note that T_c scales with r_c for $r_c < 10$ nm, while for $r_c > 10$ nm, T_c saturates to the maximum value about 90 K. We found also a corresponding correlation between the reduction of T_c and the increase of ρ_{ab} , discussed at length

elsewhere [7]. We note that the reduction $\partial T_c/\partial \rho_{ab} \approx -0.015$ K/mW cm is about 20 times smaller than in the case of irradiated samples, where columnar defects were created [13]. This difference also confirms that the disorder present in our films is not of the granular type. Finally, we note that our experimental value of the logarithmic derivative $\partial \ln T_c/\partial \ln \rho_{ab} \approx -0.3$ is the same as that obtained from experimental data on Nb₃Ge, Nb₃Sn and LuRh₄B₄ [14]. Quantitative account for these data was given by Kirkpatrick and Belitz's discussion of the effects of random potential in the Bardeen-Cooper-Schrieffer Hamiltonian [15]. Taking into account specific features of the cuprates, a similar physical picture could also account for our results.

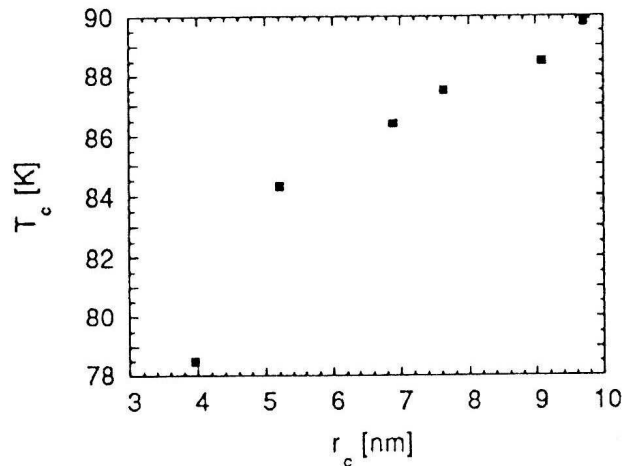


Fig. 5. The correlation between T_c and the in-plane lattice coherence length $r_c \sim 1/\Delta\vartheta$ (see also Eq. (1)) for the films considered in Fig. 2.

5. Conclusions

In conclusion, we have shown that the long range order of the lattice can be reduced in our fully doped ion-beam sputtered YBCO films by varying just one parameter: the growth temperature. We have established that the growth-induced disorder is homogeneous and we have measured a reduction of T_c as the in-plane lattice coherence length r_c is reduced by the disorder below 10 nm. This reduction is accompanied by the broadening of the resistive transition, the increase of ρ_{ab} and the appearance of a downward curvature in the temperature dependence of ρ_{ab} .

Further work is needed to nanoscopically characterize the exact type of nanoscopic defects present in the films and to study the role of the substrate(s). This should give important clues on the interplay between structural properties on the nm scale, electronic properties and the metal-insulator transition in the cuprates. Finally, we note that the Maryland group have used energy-dispersive diffraction of synchrotron-produced X-rays and analysed the microscopic inhomogeneities in YBCO single crystals [16]; their results are essentially in accordance with our analysis.

Acknowledgements

We thank J. Berrocosa for technical help. We gratefully acknowledge the financial support by the Swiss National Fund for Scientific Research and the PTT in Bern.

References

- 1) J. D. Jorgensen, S. Pei, P. Lightfoot, H. Shi, A. P. Paulikas and B. W. Veal, *Physica* **58C** (1990) 571;
- 2) H. F. Poulsen, N. H. Andersen, J. V. Andersen, H. Bohr and O. G. Mouritsen, *Phys. Rev. Lett.* **66** (1991) 465;
- 3) J. K. Burdett, *Physica* **191C** (1992) 282;
- 4) G. Deutscher, A. M. Goldman and H. Micklitz, *Phys. Rev.* **31B** (1985) 1679;
- 5) B. Dwir, *Physica* **168C** (1990) 1305;
- 6) A. Gauzzi, M. L. Lucia, B. J. Kellett, J. H. James and D. Pavuna, *Physica* **52C** (1991) 57; J. H. James, B. J. Kellett, A. Gauzzi, B. Dwir and D. Pavuna, *Applied Surface Science* **43** (1989) 393;
- 7) A. Gauzzi and D. Pavuna, *Appl. Phys. Lett.* **66** (1995) 1837;
- 8) J. Ye and K. Nakamura, *Phys. Rev.* **48B** (1993) 7554;
- 9) K. Nakamura, J. Ye and A. Ishii, *Physica* **213C** (1993) 1;
- 10) V. Holy', J. Kubena, E. Abramof, K. Lischka, A. Pesek and E. Koppensteiner, *J. Appl. Phys.* **74** (1993) 1736;
- 11) I. Wooldridge, M. A. Howson, A. Gauzzi, D. Pavuna and D. J. C. Walker, *Physica* **235-240C** (1994) 1441;
- 12) M. Gurvitch and A. T. Fiory, *Phys. Rev. Lett.* **59** (1987) 1337;
- 13) J. Giapintzakis, D. M. Ginsberg, M. A. Kirk and S. Ockers, *Phys. Rev. B* **50** (1994) 15967;
- 14) R. C. Dynes, J. M. Poate, L. R. Testardi, A. R. Strom and R. H. Hammond, *IEEE Trans. Magn.* **13** (1977) 640;
- 15) T. R. Kirkpatrick and D. Belitz, *Phys. Rev. Lett.* **68** (1992) 3232;
- 16) E. F. Skelton et al., *Science* **263** (1994) 1416.

HOMOGENI NERED REŠETKE I SUPRAVODLJIVA SVOJSTVA
YBa₂Cu₃O_{6.9} TANKIH SLOJEVA

Raspravlja ju se sistematske promjene supravodljivih svojstava tankih slojeva YBa₂-Cu₃O_{6.9} sa homogenom neuređenošću rešetke koja je uzrokovana mijenjanjem temperature rasta. T_c se smanjuje s porastom neuređenosti, dok širina otpornog prijelaza i otpornost normalnog stanja rastu. Na osnovi širenja $\Delta\vartheta$ difrakcijskih $\langle 005 \rangle$ krivulja ocijenili smo karakterističnu duljinu neuređenosti. Potiskivanje supravodljivosti i normalna vodljivost razmjerne su $\Delta\vartheta$ i pojavljuju se za duljine koherencije u-ravnini $r_c \approx 1/\Delta\vartheta$ manje od oko 10 nm.